Damage Detection and Characterization in Smart Material Structures [*] [†]

H.T. Banks and Y. Wang
Center for Research in Scientific Computation
North Carolina State University
Raleigh, NC 27695-8205

November, 1993

---

[*] Invited Lecture, International Conference on Control and Estimation of Distributed Parameter Systems, Vorau, Austria, July 18-24, 1993.

[†] Research supported in part by the Air Force Office of Scientific Research under grants AFOSR F49620-93-1-0198 and AFOSR F49620-93-1-0280. Part of this research was carried out while both authors were visiting scientists at the Institute for Computer Application in Science and Engineering (ICASE), NASA Langly Research Center, which is supported by NASA under Contract Nos. NAS1-18605 and NAS1-19480.

1 Introduction

It has been known for some time that damage such as cracks, corrosions, and delaminations in a structure produces changes in mass, stiffness, damping and other characteristics and material parameters in dynamic response models for the structure. Our focus in this paper is the development of vibration response ideas for piezoceramic based smart material structures in which self-testing nondestructive evaluation (NDE) techniques may be employed. There are several ways to formulate and analyze concepts and questions related to this quest. One could use the co-called "method-of-maps" as done in the thermal based tomography techniques of [BK1, BK2, BKW] wherein the damaged physical domain (the damaged beam, plate, elastic structure) is mapped into a regular domain on which dynamic equations with damage dependent coefficients must hold. An alternative technique involves direct estimation of the irregular damaged domain (i.e., structures with holes, cracks, corrosions, etc.) on which the usual dynamic equations hold.

The approach we take here is, strictly speaking, neither of the above, but it is more in the spirit of the latter one; we attempt to estimate damage-related changes in actual physical parameters (stiffness, damping) based on changes in physical geometry and characteristics.

Most of the previous efforts in the substantial literature on vibration related damage detection are based on modal methods (e.g. [ABB, AC, ACPS, CR, IC, S]). The basis for such methods is that damage produces a decrease in dynamic stiffness EI. This decrease in turn produces decreases in natural frequencies for an undamped simple beam (recall the eigenvalues are given by $\lambda \sim \sqrt{EI/\rho A}$ where A is the cross sectional area of the beam and ρ is the mass density). While modal based methods may have certain advantages (e.g., they are simple if they do work, they can be used in development of rank-ordering of fractional eigenfrequency shift schemes that are reportedly insensitive to the magnitude of the damage[ABB]), modal based methods possess a number of major disadvantages. First of all, some of the modal based method investigations (e.g. [CR]) provide a strong argument for including geometry of the damage in any NDE testing scheme, something which is not easily done in frequency based methods. Indeed, mode and frequency charaterizations are not so simple in variable structure systems; there is ample evidence (e.g. see [S]) that one should not use modal methods based on uniform undamped simple beams or plates as is often done in the engineering literature in addressing damage assessment methodologies. Since material parameters are most properly considered as spatially dependent quantities with damage manifested by changes in geometry (and hence in the spatial dependence of these parameters), it is unlikely that any rigorous theoretical basis for modal based methods for variable material structures will emerge. But perhaps the most serious objection to modal based methods resides in the fact that modal based methods have been shown to be highly unreliable (indeed inadequate! - see [BI] and the references therein) for estimation of variable material parameters such as damping in composite material structures.

In light of the above comments, a question of rather great interest then is: can one develop analytically sound, non-modal based self-excitation/self-sensing methods for detection and characterization (geometrical and quantitative) of damage in smart material structures? Here we address this question in the context of embedded piezoceramic structures.

For an embedded piezoceramics smart material damage detection and characterization methodology, there are several distinct requirements. These include:

(a) One must be able to *estimate reliably* (repeatable across experiments) the *variable structure material parameters* of a piezoceramic loaded structure. This must be done using piezo actuation and sensing with accuracy comparable to that achievable with standard actuating (impulse hammers, solenoidal actuators) and sensing (accelerometers, strain gauges, laser vibrometers) devices in non-smart material testing schemes.

(b) One must be able to use the actuation and sensing properties of the piezoceramics to *excite the structure and analyze the response* (in a single experiment) for a reliable methodology that is the basis of self-excitation/self-sensing.

(c) One must be able to *detect and characterize damage via vibration self-excitation/ self-sensing* that relies only on the input/output signals for the piezoceramics.

In this paper we address each of these requirements in the context of a piezoceramic loaded beam. This particular structure is sufficiently representative to make a compelling case for feasibility of the ideas we propose. In Section 2 below, we summarize a rigorous theoretical well-posedness and approximation foundation for the distributed parameter identification methodology that is the focus of our recent efforts. This is followed by Section 3 in which we detail results from experiments and computations that provide a favorable comparison for piezo actuating/sensing with standard methods (requirement (a) above). We then present experimental/computational findings on self-excitation/self-sensing capabilities of piezoceramic loaded beams. These findings suggest that requirement (b) above can indeed be satisfied.

Finally, in Section 4 we offer preliminary simulation findings on the use of vibration experiments to detect and characterize (geometrically) the extent of several types of damage in a beam using piezo actuation and sensing. Experimental verification of these positive findings with regard to requirement (c) is currently underway.

2 Distributed parameter identification methodology

The system we consider here is a cantilevered beam with piezoelectric ceramic patches for actuation and sensing. Our choice of structure is motivated by its simplicity and its representative nature. This configuration has also been well studied by conventional approaches such as finite element methods and provides a standard test bed model for comparison. The structure and model reveal the difficulties and possibilities inherent in developing models and methods for more complex structures containing damages.

We consider a cantilevered Euler-Bernoulli beam of length ℓ fixed at $x = 0$ and free at $x = \ell$. The transverse vibrations $y = y(t, x)$ are described by the system

$$\begin{aligned} &\rho(x)\frac{\partial^2 y}{\partial t^2}(t,x) + \gamma\frac{\partial y}{\partial t}(t,x) + \frac{\partial^2 M}{\partial x^2}(t,x) = \tilde{f}(t,x) \qquad 0 < x < \ell,\ t > 0, \\ &y(t,0) = \frac{\partial y}{\partial x}(t,0) = 0, \quad M(t,\ell) = \frac{\partial M}{\partial x}(t,\ell) = 0, \end{aligned} \tag{1}$$

where $\rho(x)$ is the linear mass density, γ is the coefficient of viscous (air) damping, $M(t, x)$ is the internal moment and $\tilde{f}(t, x)$ represents the external loads. For a simple Euler-Bernoulli beam with Kelvin-Voigt or strain rate damping, the internal moment is composed of two components representing resistance to bending (with coefficient $EI(x)$) and damping (with coefficient $c_D I(x)$):

$$M(t,x) = EI(x)\frac{\partial^2 y}{\partial x^2}(t,x) + c_D I(x)\frac{\partial^3 y}{\partial x^2 \partial t}(t,x). \tag{2}$$

If piezoelectric elements are bonded to the beam in a configuration to produce (or sense) only bending, we have an actuator contribution $M_p(t, x)$ in the form of an input moment (or voltage output proportional to the accumulated strain in the element). For a pair of piezoelectric actuators located between x_1 and x_2 on opposite sides of the beam excited by a voltage $u(t)$ in an out-of-phase manner (see [BSW, CA, CFW, DFR, FC]), this moment term has the representation

$$M_p(t,x) = K_B\{H(x - x_1) - H(x - x_2)\}\, u(t) \tag{3}$$

where $H(x)$ is the Heaviside or unit step function and K_B is a piezoelectric material parameter depending on the material piezoelectric properties as well as geometry. When the moment in (3) is added to that of (2) and substituted into (1), we obtain the model

$$
(4)\quad \begin{aligned}
&\rho\frac{\partial^2 y}{\partial t^2}+\gamma\frac{\partial y}{\partial t}+\frac{\partial^2}{\partial x^2}\Big(EI\frac{\partial^2 y}{\partial x^2}+c_D I\frac{\partial^3 y}{\partial x^2\partial t}\Big)\\
&\qquad = K_B\left(\frac{d}{dx}\delta(x-x_2)-\frac{d}{dx}\delta(x-x_1)\right)u(t)+\tilde f(t,x)\\
&y(t,0)=\frac{\partial y}{\partial x}(t,0)=0,\quad M(t,\ell)=\frac{\partial M}{\partial x}(t,\ell)=0
\end{aligned}
$$

where δ is the Dirac delta function. This is formally equivalent to the equation in weak or variational form (we replace partial derivatives in time by subscript t and space by superscript $'$)

$$
(5)\quad \begin{aligned}
&\langle \rho y_{tt}+\gamma y_t,\phi\rangle+\langle EI\,y''+c_D I\,y_t''+K_B(H_1-H_2)\,u(t),\phi''\rangle=\langle\tilde f(t,x),\phi\rangle\\
&y(t,0)=y'(t,0)=0,
\end{aligned}
$$

for sufficiently smooth functions ϕ satisfying $\phi(0)=\phi'(0)=0$. Here H_i is the shifted Heaviside function $H_i(x)=H(x-x_i)$, $i=1,2$ and $\langle\cdot,\cdot\rangle$ is the usual L_2 inner product.

For the same configuration, when the beam is under deformation (bending), the generated charges in terms of voltage across the piezoelectric sensors has the expression (see [DIG])

$$
K_s\int_{x_1}^{x_2}\frac{\partial^2 y}{\partial x^2}(t,x)dx=K_s\Big(\frac{\partial y}{\partial x}(t,x_2)-\frac{\partial y}{\partial x}(t,x_1)\Big)
$$

where K_s is a sensor constant which is also a piezoelectric material properties and geometry related quantity.

The system (4) is a formal representation of the dynamics of a damped beam with piezoelectric actuators. To develop computational techniques (e.g., finite elements) based on rigorous convergence arguments, it is necessary to first have a precise formulation of this system.

We start with an abstract formulation. Let V and H be complex Hilbert spaces satisfying $V\hookrightarrow H=H^*\hookrightarrow V^*$ (see [W] for the construction of this Gelfand triple), where we denote their topological duals by V^* and H^*, respectively. Let Q be the admissible parameter set. The general second order system we consider here is given by

$$
(6)\quad \begin{aligned}
&\langle\ddot y(t),\psi\rangle_{V^*,V}+\sigma_1(q)(y(t),\psi)+\sigma_2(q)(\dot y(t),\psi)=\langle f(t),\psi\rangle_{V^*,V}\quad\text{for }\psi\in V,\\
&y(0)=y_0,\quad \dot y(0)=y_1.
\end{aligned}
$$

Here we use $\langle\cdot,\cdot\rangle_{V^*,V}$ to denote the usual [W] duality product. The term $\sigma_1(q)$ and $\sigma_2(q)$ are parameter dependent sesquilinear forms on V satisfying V-ellipticity and

V-continuity conditions. That is, we assume that $\sigma_1(q)$ and $\sigma_2(q)$ satisfy

$$Re\,\sigma_i(q)(\phi,\phi) \geq k_i|\phi|_V, \tag{7}$$

$$|\sigma_i(\phi,\psi)| \leq c_i|\phi|_V \cdot |\psi|_V, \qquad i=1,2 \tag{8}$$

for $k_i, c_i > 0,\ \phi,\psi \in V$. Under weak assumptions on f, the system (6) has a unique solution.

Theorem 1 *If the sesquilinear forms σ_1 and σ_2 satisfy conditions* (7) *and* (8) *with σ_1 symmetric and $f \in L_2((0,T),V^*)$, then, for each $w_0 = (y_0,y_1) \in \mathcal{H} = V \times H$, the initial value problem* (6) *has a unique solution $w(t) = (y(t),\dot{y}(t)) \in L_2((0,T),V\times V)$. Moreover, this solution depends continuously on f and w_0 in the sense that the mapping $\{w_0,f\} \to w = (y,\dot{y})$ is continuous from $\mathcal{H}\times L_2((0,T),V^*)$ to $L_2((0,T),V\times V)$.*

For a detailed proof of this theorem see [BIW].

Returning to our beam problem, we define the sesquilinear forms by

$$\sigma_1(q)(y,\phi) = \langle EI\,y'',\phi''\rangle_{L_2} \tag{9}$$

$$\sigma_2(q)(\dot{y},\phi) = \langle c_D I\,\dot{y}'',\phi''\rangle_{L_2} + \langle\gamma\dot{y},\phi\rangle_{L_2} \tag{10}$$

with the spaces defined by $V = H_L^2(0,\ell) = \{\phi \in H^2(0,\ell)\,|\,\phi(0) = \phi'(0) = 0\}$ and $H = L_2(0,\ell)$ with weighted inner product $\langle\cdot,\cdot\rangle_H = \langle\rho\cdot,\cdot\rangle_{L_2}$. We assume throughout that $\rho \in L_\infty(0,\ell)$ with $\rho(x) \geq \alpha$ for some $\alpha > 0$. The term $f(t) = f(t,x)$ is given by

$$f(t,x) = \frac{1}{\rho}K_B(H''(x-x_2) - H''(x-x_1))u(t) + \frac{1}{\rho}\tilde{f}(t,x),\quad 0 \leq x,x_1,x_2 \leq \ell, \tag{11}$$

where $f(t,x)$ belongs to the dual space (see [W]) $V^* = \left(H_L^2(0,\ell)\right)^*$ (we assume that $\tilde{f}(t,x) \in V^*$ which is a weak assumption on $\tilde{f}$). If both $|EI(\cdot)|_{L_\infty} \geq \alpha$ and $|c_D I(\cdot)|_{L_\infty} \geq \alpha$ for some $\alpha > 0$, then σ_1 and σ_2 are V-elliptic and continuous with σ_1 symmetric; hence by Theorem 1 our beam equation is well posed for $f(t,x)$ given by (11).

The parameter estimation problems can be stated in terms of finding parameters which give the best fit of the parameter dependent solutions of the partial differential equations to the observation data for response of the system to various excitations. In our case, the parameters to be estimated include beam mass density $\rho(x)$, stiffness coefficient $EI(x)$ as well as damping parameters $c_D I(x)$, γ and piezoelectric material parameters K_B, K_s. Let the collection of unknown parameters be denoted by $q = (\rho(x), EI(x), c_D I(x), \gamma, K_B, K_s)$. For given observations $\{z_i\}$ corresponding to measurements at times t_i as obtained in most practical cases, we consider the least squares estimation problem of minimizing over $q \in Q$ the least squares functional

$$J(y, z; q) = \left| \tilde{C}_2 \Big(\tilde{C}_1 \{ y(t_i, \cdot; q) \} - \{ z_i \} \Big) \right|^2, \tag{12}$$

where $\{y(t_i, \cdot; q)\}$ are the parameter dependent weak solutions of (4) or (6) evaluated at each time t_i, $i = 1, 2, \cdots, \bar{N}$ and $| \cdot |$ is an appropriately chosen Euclidian norm. The set Q is some admissible parameter set. The operator $\tilde{C}_1$ may have several forms depending on the type of sensors being used. When the collected data are displacement, velocity, or acceleration at a point $\bar{x}$ on the beam, we minimize

$$J_\nu(q) = \sum_{i=1}^{\bar{N}} \left| \frac{\partial^\nu y}{\partial t^\nu}(t_i, \bar{x}; q) - z_i \right|^2, \tag{13}$$

for $\nu = 0, 1, 2$, respectively. In this case the operator $\tilde{C}_1$ involves differentiation (either $\nu = 0, 1$ or 2 times, respectively) with respect to time followed by pointwise evaluation in t and x. When a piezoelectric sensor is used, the functional to be minimized is

$$J_p(q) = \sum_{i=1}^{\bar{N}} \left| K_s \Big(\frac{\partial y}{\partial x}(t_i, x_2; q) - \frac{\partial y}{\partial x}(t_i, x_1; q) \Big) - z_i \right|^2, \tag{14}$$

for the piezoelectric elements being located on the beam between x_1 and x_2. Here $\{z_i\}$ are the measured voltages across the piezoelectric elements.

The operator $\tilde{C}_2$ may be the identity (corresponding to time domain identification procedures as in (13) and (14)) or the Fourier transform (corresponding to identification in the frequency domain). If the identification is carried out in the frequency domain and the operator $\tilde{C}_2$ is a Fourier transform operator, the corresponding cost functional is given by

$$\hat{J}(q) = \sum_{\ell=1}^{\bar{N}_M} \left(\epsilon_1 \left| \mathrm{f}_{k_\ell^y}(q) - \mathrm{f}_{k_\ell^z} \right|^2 + \epsilon_2 \sum_{j=-n_\ell}^{N_\ell} \left| \, |U(k_\ell^y + j; q)| - |Z(k_\ell^z + j)| \, \right|^2 \right), \tag{15}$$

where $U(k; q)$ and $Z(k)$ are the Fourier series coefficients of $\tilde{C}_1\{y(t_i, \bar{x}; q)\}$ and $\{z_i\}$ respectively, $\mathrm{f}_{k_\ell^y}$ and $\mathrm{f}_{k_\ell^z}$ are the $(k_\ell^y)^{th}$ vibration frequency of the solution $U(k; q)$ and the $(k_\ell^z)^{th}$ frequency of the observation data $Z(k)$, ϵ_1, ϵ_2 are weighting constants, and n_ℓ, N_ℓ are certain lower and upper limits associated with the width (or the support) of the ℓ^{th} spikes. In obtaining (15), we have assumed that there are a finite and distinct number $\bar{N}_M$ ($< \bar{N}$) of "spikes", i.e. vibration frequencies, among the $Z(k)$ and the number of spikes of the solution $U(k; q)$ is the same as $\bar{N}_M$. We refer to [BW] for a detailed derivation and discussion of the cost functional (15).

The minimization in our parameter estimation problems involves an infinite dimensional state space and an infinite dimensional admissible parameter set (of functions). We thus consider Galerkin type approximations in the context of the variational formulation of (6). Let H^N be a sequence of finite dimensional subspaces of H, and Q^M be a sequence of finite dimensional sets approximating the parameter set Q. We define the orthogonal projections $P^N : H \to H^N$ of H onto H^N. Then a family of approximating estimation problems with finite dimensional state spaces and parameter sets can be formulated by seeking $q \in Q^M$ which minimizes

$$J^N(y^N, z; q) = \left| \tilde{C}_2 \left(\tilde{C}_1 \{ y^N(t_i, \cdot; q) \} - \{ z_i \} \right) \right|^2, \tag{16}$$

where $y^N(t; q) \in H^N$ is the solution to the finite dimensional approximation of (6) given by

$$\begin{aligned} &\langle \ddot{y}^N(t), \psi \rangle_{V^*,V} + \sigma_1(q)(y^N(t), \psi) + \sigma_2(q)(\dot{y}^N(t), \psi) = \langle f(t), \psi \rangle_{V^*,V} \\ &y^N(0) = P^N y_0, \quad \dot{y}^N(0) = P^N y_1, \end{aligned} \tag{17}$$

for $\psi \in H^N$.

For the parameter sets Q and Q^M, and state spaces H^N, we make the following hypotheses:

(H1) The sets Q and Q^M lie in a metric space $\tilde{Q}$ with metric d with Q, Q^M compact in this metric and there is a mapping $i^M : Q \to Q^M$ so that $Q^M = i^M(Q)$. Furthermore, for each $q \in Q, i^M(q) \to q$ in $\tilde{Q}$ with the convergence uniform in $q \in Q$;

(H2) The finite dimensional subspaces H^N satisfy $H^N \subset V$ as well as the approximation properties: For each $\psi \in V$, $|\psi - P^N \psi|_V \to 0 \quad$ as $N \to \infty$.

In addition to (uniform in Q) ellipticity and continuity conditions (7) and (8), the sesquilinear forms $\sigma_1(q)$ and $\sigma_2(q)$ are assumed to be defined on Q and satisfy the continuity-with-respect-to-parameter conditions

$$| \sigma_i(q)(\phi, \psi) - \sigma_i(\tilde{q})(\phi, \psi) | \le \gamma_i \, d(q, \tilde{q}) \, |\phi|_V \, |\psi|_V, \qquad i = 1, 2, \tag{18}$$

for $\phi, \psi \in V$ and $q, \tilde{q} \in Q$ where the constants γ_1, γ_2 depend only on Q.

Solving the approximate estimation problems involving (16) and (17), we obtain a sequence of estimates $\{\bar{q}^{N,M}\}$. To obtain parameter estimate convergence and continuous dependence (with respect to the observations $\{z_i\}$) results, it has been shown in [B], [BK3] and [BWI] that it is suffices, under the assumption that Q is a compact set, to argue that for arbitrary $\{q^{N,M}\} \in Q$ with $q^{N,M} \to q \in Q$, we have

$$\tilde{C}_2 \tilde{C}_1 y^N(t; q^{N,M}) \to \tilde{C}_2 \tilde{C}_1 y(t; q) \tag{19}$$

for each t.

The following theorem and corollary establish the convergence (19) for all forms of $\tilde{C}_1$, $\tilde{C}_2$ that are of interest to us here.

Theorem 2 *Suppose that* Q, Q^M *satisfy (H1) and* H^N *satisfies (H2). Assume that the sesquilinear forms* $\sigma_1(q)$ *and* $\sigma_2(q)$ *satisfy* (7), (8), (18). *Furthermore, assume that*

$$q \to f(t;q) \text{ is continuous from } Q \text{ to } L_2((0,T),V^*).$$

Let $q^{N,M}$ *be arbitrary in* Q *such that* $q^{N,M} \to q$ *in* Q*; then for* $t > 0$ *as* $N, M \to \infty$ *we have*

$$\frac{\partial^\nu y^N}{\partial t^\nu}(t;q^{N,M}) \to \frac{\partial^\nu y}{\partial t^\nu}(t;q) \qquad \text{in } V \text{ norm, for } \nu = 0,1,2,$$

where y^N, $\dot{y}^N$ *are the solutions to* (17) *and* y, $\dot{y}$ *are the solutions to* (6).

Furthermore we have

Corollary 2.1 *Under the assumptions of Theorem 2, we have as* $N, M \to \infty$

$$\frac{\partial y^N}{\partial x}(t;q^{N,M}) \to \frac{\partial y}{\partial x}(t;q) \qquad \text{in } H^1 \text{ norm, for } t > 0,$$

$$\sum_{\ell=1}^{\bar{N}_M} \left(\epsilon_1 \left| f_{k_\ell^{y^N}}(q^{N,M}) - f_{k_\ell^y(q)} \right|^2 + \epsilon_2 \sum_{j=-n_\ell}^{N_\ell} \left| |U^N(k_\ell^{y^N} + j; q^{N,M})| - |U(k_\ell^y + j; q)| \right|^2 \right) \to 0,$$

where $U^N(k;q^{N,M})$ *and* $U(k;q)$ *are the Fourier series coefficients for* $\tilde{C}_1\{y^N(t;q^{N,M})\}$ *and* $\tilde{C}_1\{y(t;q)\}$*, respectively.*

The corollary follows from Theorem 2. For a detailed proof when $\tilde{C}_2$ is the Fourier transform see [BWI]. For the proof of Theorem 2, we refer the reader to [BWIS] for the cases $\nu = 0, 1$ and [BR] for the case $\nu = 2$.

We have outlined a framework for methods to carry out parameter identification for distributed parameter systems in both the time domain and the frequency domain. The motivation for introducing a frequency domain technique is that the time domain techniques give poor results when the observations contain several vibration modes and the initial guesses for parameters are not close to the optimal ones ([WA]). In such a situation we use a hybrid of these two methods: we iterate in a frequency domain formulation to obtain a reasonable initial parameter estimate for the time domain formulation which is then used to complete the identification procedure.

In Theorem 2, we presented convergence results allowing approximation of the parameter set. This form of the theoretical foundation provides a sound necessary basis for the detection and quantification of damage in structures since damage affects the dynamic behavior of systems in terms of changes in the system parameters such as ρ and I.

In concluding this section we make further comments related to the various allowable forms of the operator $\tilde{C}_1$. The flexibility in the choice of $\tilde{C}_1$ and hence flexibility in the choice of sensors in the above theoretical framework makes it possible to carry out cross experiments to test the reliability of our methods. Even more important, this flexibility in our method enables us to use smart materials to carry out damage detection by employing only piezoelectric materials in actuating and sensing for the structure.

3 Quantitative and Experimental Results

In implementing the computational method outlined in Section 2, we chose cubic splines as the basis elements. The finite dimensional space H^N is defined as the span of the basis set for $S^N_{3,B}(0,\ell)$ (the cubic B-splines corresponding to mesh size ℓ/N - see [P]) with the basis set modified to satisfy the essential boundary conditions $\phi(0) = \phi'(0) = 0$. The finite dimensional space H^N constructed in this manner satisfies hypothesis (H2) (for details see [BWIS]). The dimension of the resulting approximation space is $N+1$. For our calculations we chose $N = 10$, since the eigenvalues of this approximate finite dimensional system become stable at and after $N = 10$ in the sense that the eigenvalues did not change significantly as N increases beyond 10.

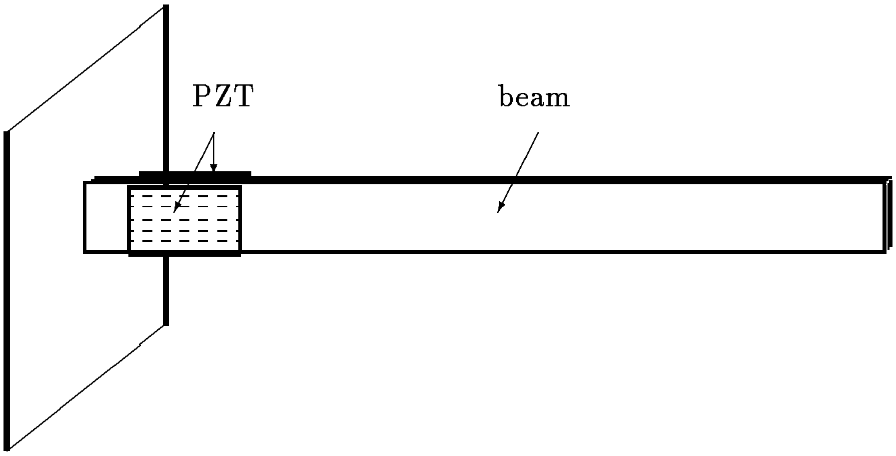

Figure 3.1: Test beam with piezoceramic patches.

In the numerical examples we present next, an undamaged beam with two

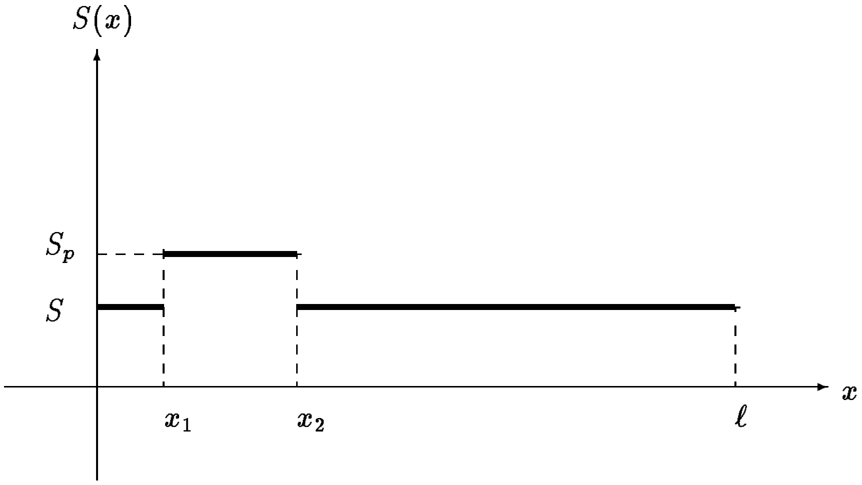

Figure 3.2: $\rho(x)$, $EI(x)$, $c_D I(x)$ function shape $S(x)$.

attached piezoceramic patches (PZT) as shown in Figure 3.1 was used as a test structure to demonstrate the consistency of identification results for our computational method across different excitation and sensing mechanisms. To accurately model the geometry of the structure, we assumed that the mass density, stiffness and Kelvin-Voigt damping coefficients are piecewise constant functions as depicted in Figure 3.2. These assumptions were subsequently verified to be most reasonable. For the choice of parameters $q = (\rho(x), EI(x), c_D I(x), \gamma, K_B, K_s)$, we take the parameter space $\tilde{Q}$ to be $[L_\infty(0,\ell)]^3 \times \mathbb{R}^3$, and the parameter set Q to be a uniformly bounded collection of piecewise constant functions each having jump discontinuities at most at x_1 and x_2. If we choose the mapping i^M as the identity, then hypothesis (H1) is satisfied.

Experiments with a test beam as depicted in Figure 3.1 were carried out at the Mechanical Systems Laboratory, then located at the State University of New York at Buffalo (now at Virginia Polytechnic Institute and State University). The measured dimensions of the actual structure are given in Table 3.1 and the handbook values for the physical characteristics of this aluminum (2024-T4) beam/piezo (G-1195 PZT ceramic) structure are given in Table 3.2. In the tables the subscripts indicate the materials: b for beam and p for piezoceramic, ℓ is length, w is width, t is thickness, E is the Young's modulus, and ρ is the mass density. The patches were bonded to the beam on the opposite sides of the beam at the same position.

The beam was clamped at $x = 0$. The piezoceramic patches were placed between $x_1 = 2.54cm$ and $x_2 = 8.89cm$ (or $1''$ and $3.5''$ respectively) on the beam. The time response data and input signal from the experimental beam were obtained

Unit	ℓ_b	w_b	t_b	ℓ_p	w_p	t_p
Metric	$45.73cm$	$2.03cm$	$0.16cm$	$6.37cm$	$2.03cm$	$0.0254cm$
English	$18''$	$0.8''$	$.0625''$	$2.5''$	$0.8''$	$0.01''$

Table 3.1: Dimension of the beam and piezoceramic patch.

Unit	E_b	ρ_b	E_p	ρ_p
Metric	$7.3 \times 10^6 N/cm^2$	$2.766g/cm^3$	$6.3 \times 10^6 N/cm^2$	$7.6g/cm^3$
English	$10.6 \times 10^6 psi$	$0.1\ell b/in^3$	$9.148 \times 10^6 psi$	$0.275\ell b/in^3$

Table 3.2: Characteristics of the beam and piezoceramic patch.

using a Tektronix Analyzer (model 2600). For more detailed descriptions of the experimental setup and the parameter identification procedure, see [BWIS].

In examining the ability of our method to estimate parameters reliably, independent of the type of excitation or sensing device used, two separate experiments were performed. In the first experiment an impulse hammer was used as the input device and piezoceramic patches were used as a sensor. In the second experiment, the excitation was obtained via an input voltage to the patches and observation data was recorded from an accelerometer. At a sampling frequency of 256 Hz for 16 seconds, two modes (at 6.625 Hz and 38.375 Hz) were observed in the response in each experiment.

The results (graphs comparing the model response after ID of parameters with the experimental data) for the first identification experiment are given in Figure 3.3.

In this example, the beam was excited by an impulse force applied (via the impulse hammer) to the beam along the neutral axis at $2.54cm(1'')$ away from the clamped end. Then the forcing function in (11) becomes (since $u \equiv 0$)

$$f(t,x) = \tilde{f}(t,x)$$

with $\tilde{f}$ given by the impulse. The recorded signal exhibited a triangular shape. The voltages across the patches due to the beam vibrations were collected as observation data.

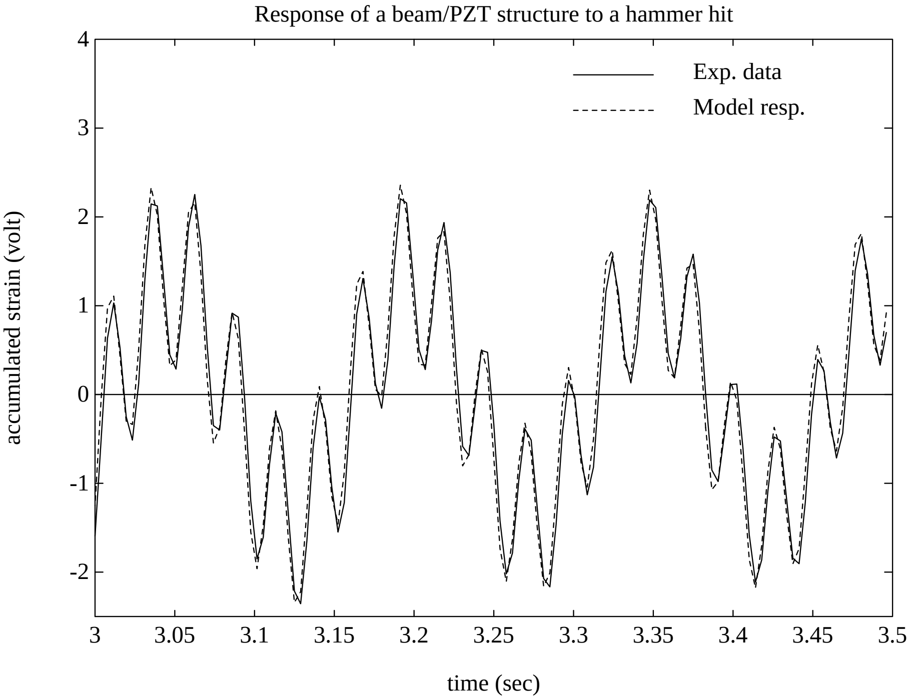

(a): Time history in [3, 3.5] seconds.

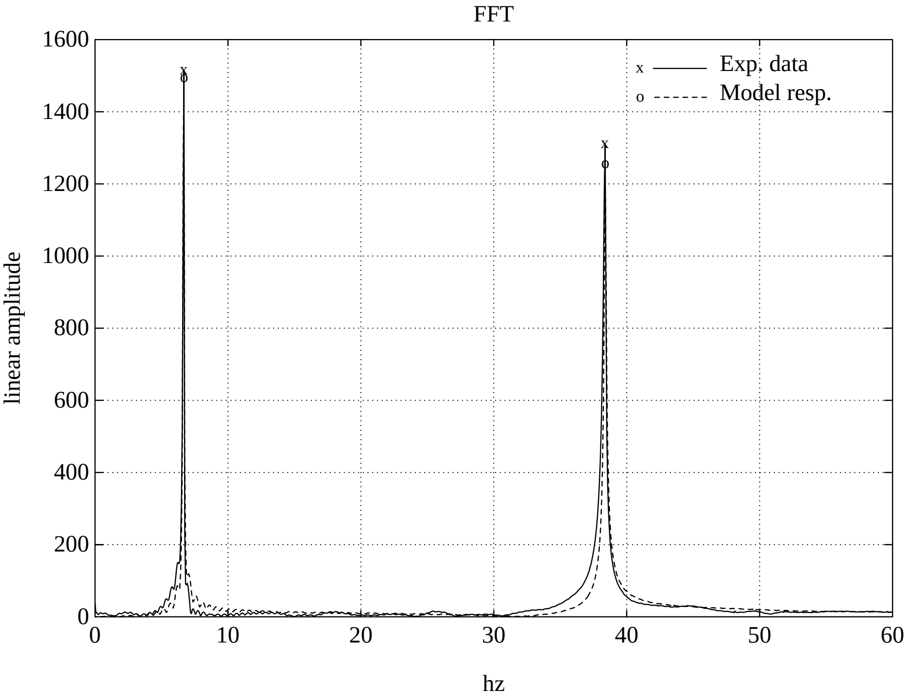

(b): Frequency content.

Figure 3.3: ID result for Experiment 1 (actuator–impulse hammer, sensor–PZT).

Exp. No.	actuator / sensor	EI		ρ		c_DI ($\times 10^{-5}$)		γ	K_s	K_B
		beam	beam + PZT	beam	beam + PZT	beam	beam + PZT			
given		0.495	1.051	0.089	0.168	—	—	—	—	—
Exp. 1	hammer /PZT	0.491	0.793	0.093	0.433	0.649	1.255	0.013	46.823	—
Exp. 2	PZT/ accel.	0.505	0.798	0.096	0.441	0.637	1.275	0.013	—	0.0175

Table 3.3: Given and estimated structural parameters for Experiments 1 and 2.

In the second experiment, a narrow triangular shaped voltages (approximating an impulse) was applied to the patches to excite the beam. The piezoceramic patches were excited out-of-phase so as to produce pure bending moments. Hence the input function is

$$f(t,x) = K_B(H''(x-x_2) - H''(x-x_1))u(t).$$

An accelerometer weighing 0.5 gram, located at $\bar{x} = 2.14cm(0.844'')$ was used as the sensor. The parameter identification results are shown in Figure 3.4 where the data time history is compared to the model response corresponding to the best-fit parameters.

A summary of the estimated parameters is given in Table 3.3, where the units are for EI in $N \cdot m^2$, ρ in kg/m, c_DI in $s \cdot N \cdot m^2$, γ in $s \cdot N/m^2$, K_s in v, and K_B in $N \cdot m/v$. The measured and handbook quantities are listed in the table as "given" values; these were calculated according to the following equations

Exp. No.	actuator / sensor	EI		ρ		c_DI ($\times 10^{-5}$)		γ	K_s	K_B
		beam	beam + PZT	beam	beam + PZT	beam	beam + PZT			
given		0.495	1.051	0.089	0.168	—	—	—	—	—
Exp. 3	PZT /PZT	0.505	0.796	0.095	0.483	0.697	1.275	0.013	46.823	0.0196

Table 3.4: Given and estimated structural parameters for Experiment 3.

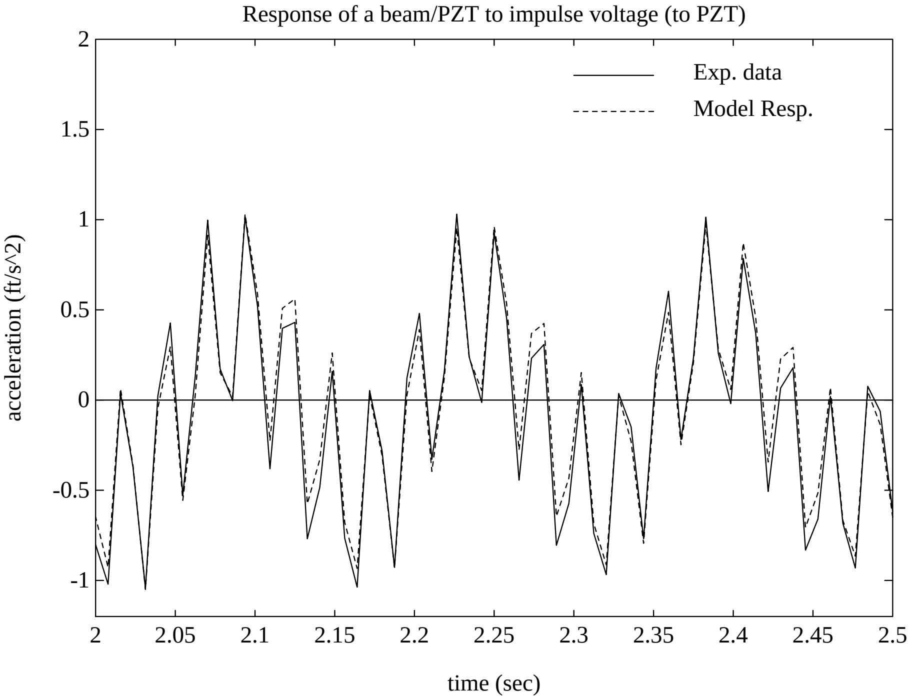

(a): Time history in [3, 3.5] seconds.

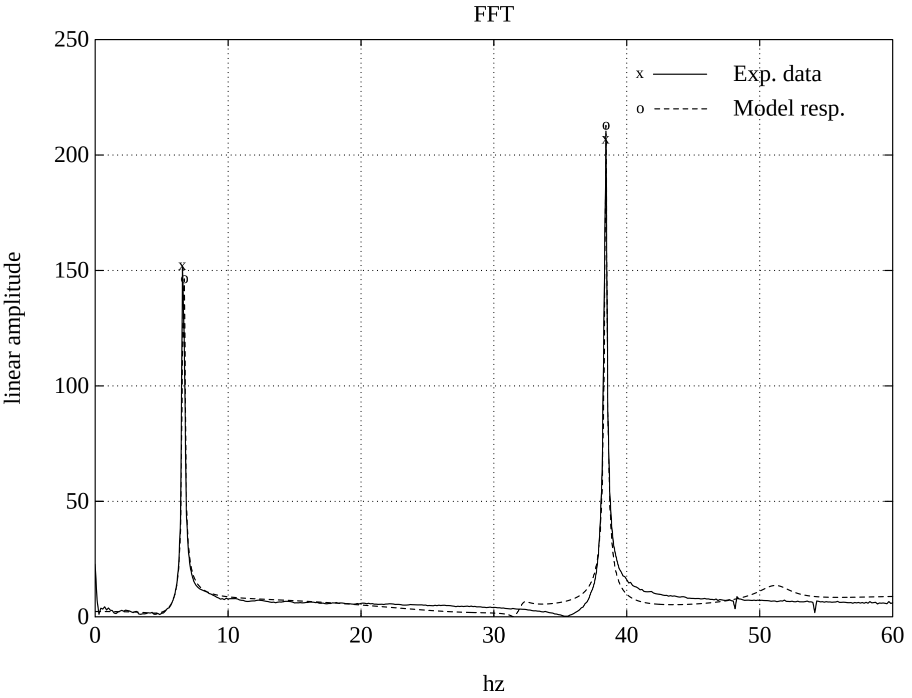

(b): Frequency content.

Figure 3.4: ID result for Experiment 2 (actuator–PZT; sensor–accelerometer).

$$\rho(x) = \rho_b t_b w_b + 2\rho_p t_p w_p \chi_p(x) \tag{1}$$

$$EI(x) = \frac{1}{12} t_b^3 w_b E_b + \frac{2}{3}\left[(\frac{t_b}{2} + t_p)^3 - (\frac{t_b}{2})^3\right] w_p E_p \chi_p(x) \tag{2}$$

where χ_p is a characteristic function given by

$$\chi_p(x) = \begin{cases} 1 & x_1 < x < x_2 \\ 0 & \text{otherwise.} \end{cases} \tag{3}$$

We next sought to demonstrate the capability of piezoelectric materials in smart structures (specifically in the area of self-evaluation of structures). We designed and performed an experiment on the same beam in which the piezoceramic patches were used as actuator and sensor in self-identification of material parameters. In this third experiment, the structure was excited by an input of sinusoidal voltage, out-of-phase, to the PZT patches for a time period of $[0, t_0)$ and was left to free vibrate for $t \geq t_0$. The circuit setup for this experiment is depicted in Figure 3.5.

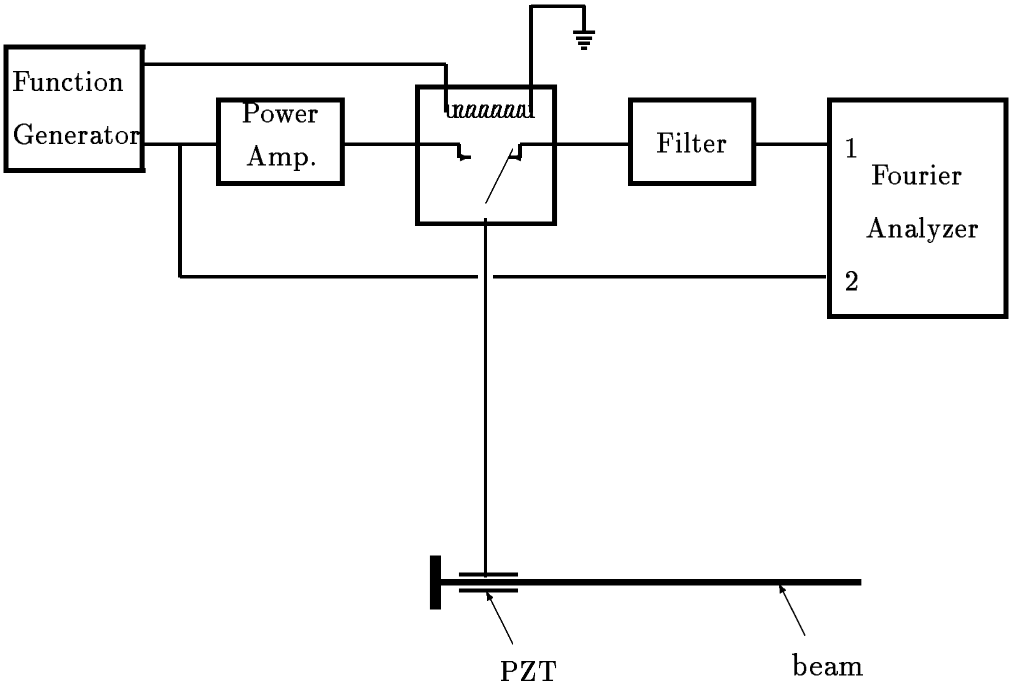

Figure 3.5: Circuit for the experiment using PZT as actuator/sensor.

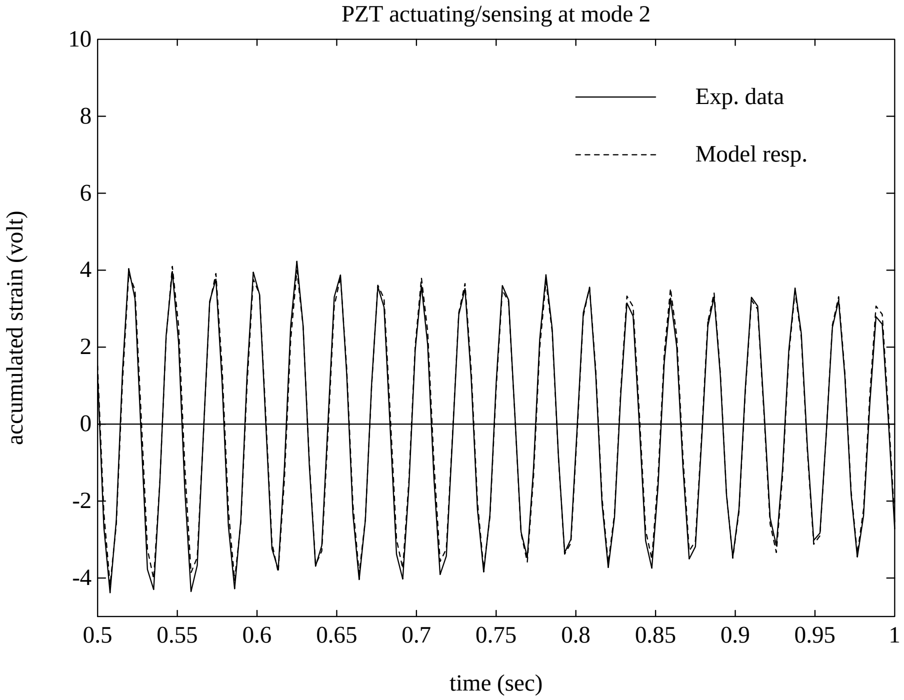

(a): Time history in [0.5, 1.0] seconds.

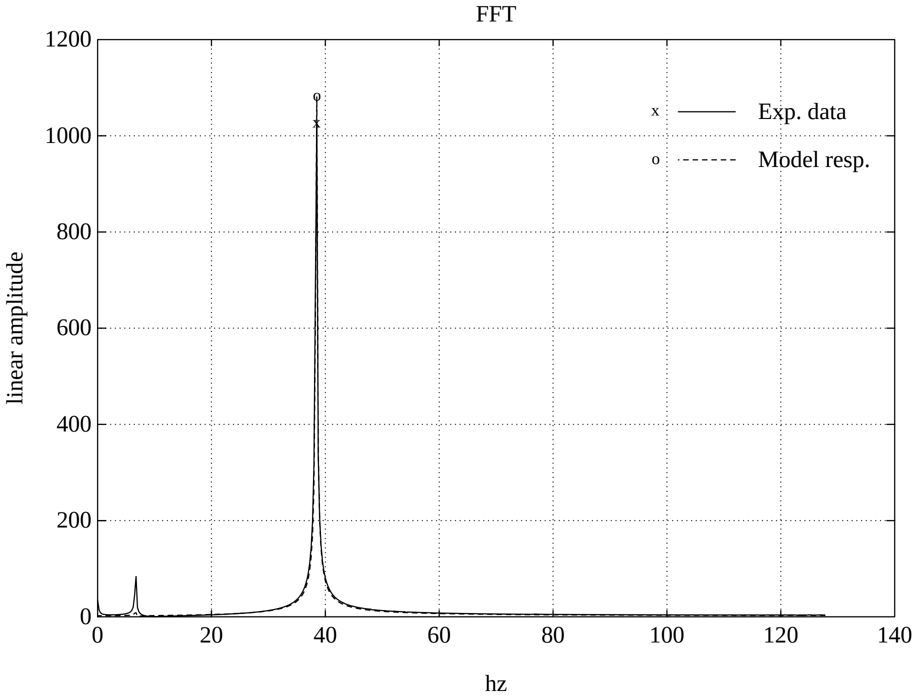

(b): Frequency content.

Figure 3.6: ID result for Experiment 3 (actuator–PZT; sensor–PZT).

The accumulated strain in form of a voltage across the patches was recorded for approximately 14 seconds. The sample rate was 256 Hz and the excitation frequency was 38.25 Hz; this is approximately the second vibration mode of the composite structure (beam with bonded patches). The estimated parameters are reported in Table 3.4 in which the units are the same as those given for Table 3.3. Comparison of the model response (after parameter ID) to the experimental data is shown in Figure 3.6.

It can be observed that identification results for $\rho(x), x_1 < x < x_2$, in all three examples yield values that are substantially larger than the given one. One explanation for this is that equation (1) is simply a superposition of linear mass densities of the beam and the patches which ignores the mass of the bonding glue and the conducting copper foil.

In all our parameter estimation procedures, we adopted a so-called hybrid method (mentioned previously) , wherein we started with the cost function (15) (the cost function corresponding to frequency domain data) and then switched to (13) or (14) (time domain data). Our experience on these and numerous other inverse problems reveal that parameter identification in time domain is more sensitive and accurate if the initial guesses of parameters are close to the optimal ones. On the other hand, parameter identification in the frequency domain will yield quick and rough estimates with the resulting parameters in a neighborhood of the optimal values.

From the above reported results, we can conclude that the methodology outlined in the previous section yields theoretical, computational and experimental findings that are consistent. Moreover, it is feasible to use smart materials in nondestructive self-evaluation schemes such as presented in the next section.

4 Detection and Characterization of Damage

In our preliminary investigation of damage detection capabilities we have carried out simulation studies. The structure used in the simulation has the same dimensions and physical characteristics as the beam in Section 3. The difference is that the beam is assumed damaged by a hole. Since the beam model is based on Euler-Bernoulli theory, we assume that the center of the hole coincides with the neutral axis of the beam. Furthermore, we assume that the hole is either a circle centered at x_d with dimension r or a rectangle centered at x_d with dimension of $2r \times w_d$. With these assumptions, the functions $\rho(x)$ and $EI(x)$ can be expressed by

$$(1) \quad \rho(x) = \rho_b t_b w_b + 2\rho_p t_p w_p \chi_p(x) - \rho_b t_b (w_b - \tilde{w}) \chi_d(x)$$

$$(2)\quad EI(x) = \frac{1}{12}t_b^3 w_b E_b + \frac{2}{3}\Big[(\frac{t_b}{2} + t_p)^3 - (\frac{t_b}{2})^3\Big] w_p E_p \chi_p(x) - \frac{1}{12}t_b^3 E_b (w_b - \tilde{w})\chi_d(x)$$

where the characteristic function χ_p is the same as (3) and χ_d is given by

$$(3)\qquad \chi_d(x) = \begin{cases} 1 & x_{d_1} < x < x_{d_2} \\ 0 & \text{otherwise.} \end{cases}$$

Here $x_{d_1} = x_d - r$ and $x_{d_2} = x_d + r$, and

$$\tilde{w} = \begin{cases} w_d & \text{for a rectangular hole} \\ 2\sqrt{r^2 - (x - x_d)^2} & \text{for a circular hole.} \end{cases}$$

The Kelvin-Voigt damping function $c_D I(x)$ has the same form as (2) with E replaced by c_D. In both examples, the damage is parameterized by parameters r and x_d with w_d held fixed in the case of a rectangular hole at a value $w_d = 1.016\text{cm}(.4'')$.

In the simulations, we assumed that we knew the shape (rectangular or circular) of the damage. The damage detection (location and size of the hole) is carried out through parameter identification by fitting the solution of the model to the simulated observation data much in the same manner as described for the experimental data cases described in Section 3. Voltage measurements across the piezoceramic patches are used as observations.

The input data is a triangular (time function) voltage in a very short time period (see Figure 4.1) to simulate an impulse input. The choice of the triangular function was motivated by impulse hammer excitation records from actual experiments as reported in Section 3.

The simulated "observation data" $\{z_i\}$ were generated by solving the finite dimensional model (17). The number of finite elements was set at $N = 10$ with cubic spline basis elements. The time interval was $[0, 8]$ seconds with sampling rate 512 Hz. Parameters estimated from experimental data and given in Table 3.4 were used for the simulated test structure.

In the following two examples, one with a rectangular hole and one with a circular hole, two cases were investigated. In Case I, the simulated observation data was generated with a damaged beam (a hole in the beam) and in Case II the data was generated with a undamaged beam (without holes). In these simple preliminary tests, these simulated data sets were used without additional noise. In the parameter estimation procedures, we also used 10 finite elements (cubic splines) in solving the inverse problems.

EXAMPLE 1. We assumed there was a rectangular hole in the beam. The parameters defining the hole in the simulated data were

$$r = 0.508cm(0.2''), \quad x_d = 10.414cm(4.1'').$$

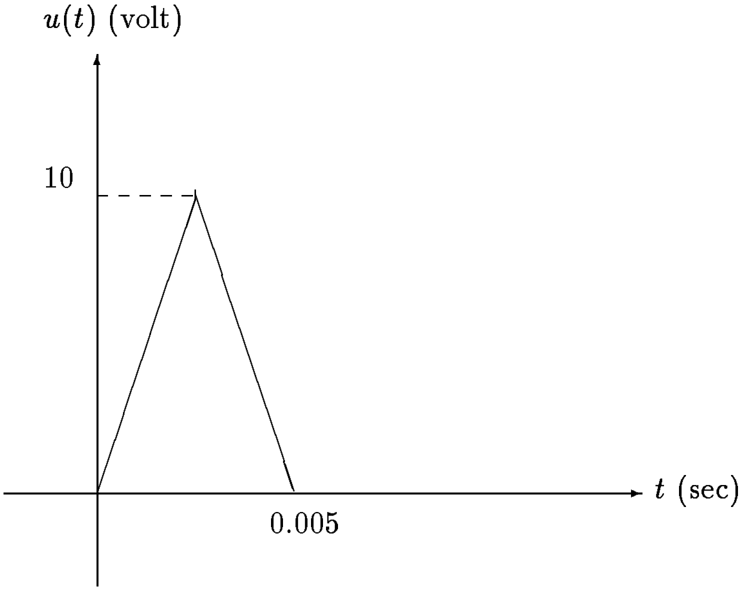

Figure 4.1: Input voltage.

The initial guesses and converged parameters are shown in Table 4.1.

EXAMPLE 2. In this example, the damage is characterized by a circular hole in the beam. The parameters for the hole were

$$r = 0.508cm(0.2''), \quad x_d = 10.414cm(4.1'').$$

The initial guesses and converged parameters are shown in Table 4.2.

As was noted, in these simulation examples we used noise free simulated observation data in the parameter estimation problems. We are currently studying the effects of noise in the data on the accuracy of the estimated parameters.

In many simulation studies found in the literature, the impulse function inputs are approximated by a smooth function, for example, $\sin^2(\alpha t)$. Our choice of a triangular shape for these input functions is in practice equivalent to the choice of a smooth function since discrete input data are used and hence smoothness of the time records does not play a role in the sampling process or the trajectories obtained.

The results reported in this section are very encouraging. These initial calculations suggest that our methods for parameter identification can reveal whether there is a damage or not. Our current efforts involve eliminating the assumed preknowledge of the shape of the damage. We also are investigating issues related to the detection and characterization of cracks in structures.

Case I.

Unit	Parameters	Initial	Final	Preassigned
Metric	$x_d(cm)$	3.048	10.414	10.414
	$r(cm)$	0.152	0.508	0.508
English	$x_d(in)$	1.2	4.1	4.1
	$r(in)$	0.06	0.2	0.2

Case II.

Unit	Parameters	Initial	Final	Preassigned
Metric	$x_d(cm)$	3.048	1.753	0
	$r(cm)$	0.152	1.592×10^{-6}	0
English	$x_d(in)$	1.2	0.69	0
	$r(in)$	0.06	6.27×10^{-7}	0

Table 4.1: Damage detection results for: Case I. damage in shape of a rectangle; Case II. no damage

Case I.

Unit	Parameters	Initial	Final	Preassigned
Metric	$x_d(cm)$	3.048	10.414	10.414
	$r(cm)$	0.152	0.508	0.508
English	$x_d(in)$	1.2	4.1	4.1
	$r(in)$	0.06	0.2	0.2

Case II.

Unit	Parameters	Initial	Final	Preassigned
Metric	$x_d(cm)$	3.048	3.315	0
	$r(cm)$	0.152	4.55×10^{-3}	0
English	$x_d(in)$	1.2	1.305	0
	$r(in)$	0.06	1.791×10^{-3}	0

Table 4.2: Damage detection results for: Case I. damage in shape of a circle; Case II. no damage

5 Concluding remarks

As we have noted in the introduction of this paper, the idea of using vibration testing as a basis for damage detection in structures is not new. However, most methods to date are based on modal techniques. In this paper we have presented a theoretical and computational non-modal framework for the identification of spatially dependent dynamic parameters in piezoceramic embedded structures using nondestructive vibration tests. This rigorous foundation permits one to use the piezoceramics to both excite and sense vibrations in a self-analysis framework that is a natural major feature of smart material structures.

Using data from beam experiments, we have demonstrated the feasibility of our approach in obtaining reliable physically meaningful dynamic parameters such as stiffness, damping, and mass density. In preliminary simulation studies on the possibility of detecting and geometrically characterizing damage such as holes, we have presented examples which suggest that such methods offer great promise. While much remains to be done in developing these ideas into general algorithms, we are most encouraged by our initial findings and are currently designing and carrying out physical experiments to support further efforts on geometric characterization of damage such as corrosions, cracks, and delaminations in composite material structures.

6 Acknowledgement

The authors would like to gratefully acknowledge continuing valuable discussions and encouragement from Dr. W. Winfree, NASA Langley Research Center, and Dr. D.J. Inman, Virginia Polytechnic Institute and State University. The authors are indebted to Dr. Inman and Dr. J. Slater (Wright State University) for their assistance and collaboration on the experimental efforts summarized in this paper and the references.

REFERENCES

[ABB] D. Armon, Y. Ben-Hain, and S. Braun, *Crack detection in beams by rank-ordering of eigenfrequency shifts*, Mechanical Systems and Signal Processing, to appear.

[AC] R.D. Adams and P. Cawley, *The location of defects in structures from measurements of natural frequencies*, J. Strain Analysis 14 (1979), pp. 49-57.

[ACPS] R.D. Adams, P. Cauley, C.J. Pye and B.J. Stone, *A vibrational technique for nondestructively assessing the integrity of structures*, J. Mech. Engr. Sci. 20 (1979), pp. 93-100.

[B] H.T. Banks, *On a variational approach to some parameter estimation problems*, in Distributed Parameter Systems (ed. by F. Kappel, et. al.), Springer Lecture Notes in Control and Information Sciences, 75 (1985), pp. 1-23.

[BI] H.T. Banks and D.J. Inman, *On damping mechanisms in beams*, ICASE Rep. #89-64 August, 1989; ASME J. Applied Mechanics 58 (1991), pp. 716-723.

[BIW] H.T. Banks, K. Ito and Y. Wang, *Well posedness for damped second order systems with unbounded input operators*, CRSC-TR93-10, North Carolina State University, June, 1993; Differential and Integral Equations, submitted.

[BK1] H.T. Banks and F. Kojima, *Boundary shape identification problems in two dimensional domains related to thermal testing of materials*, Quart. Applied Math., 47 (1989), pp. 273-293.

[BK2] H.T. Banks and F. Kojima, *Boundary identification for 2-D parabolic systems arising in thermal testing materials*, Proceedings of 27th IEEE Cong. on Dec. and Control (1988), pp.1678-1683.

[BK3] H.T. Banks and K. Kunisch, *Estimation Techniques for Distributed Parameter Systems*, Birkhaüser, Boston, 1989.

[BKW] H.T. Banks, F. Kojima, and W.P. Winfree, *Boundary estimation problems arising in thermal tomography*, CAMS Tech. Rep 89-6, University of Southern California; Inverse Problems 6 (1990), pp. 897-921.

[BR] H.T. Banks and D.A. Rebnord, *Analytic semigroups: applications to inverse problems for flexible structures*, in Differential Equations with Applications (ed. by J. Goldstein, et. al.), Marcel Dekker, 1991, pp. 21-35.

[BSW] H.T. Banks, R. Smith and Y. Wang, *The modeling of piezoceramic patch interactions with shell, plates and beams*, Quarterly of Applied Mathematics, to appear.

[BW] H.T. Banks and Y. Wang, *Parameter identification in the frequency domain*, in Progress in Systems and Control Theory: Computation and Control III, (ed. by K Bowers and J. Lund) Birkhäuser, 1993, pp. 49-62.

[BWI] H.T. Banks, Y. Wang and D.J. Inman, *Bending and shear damping in beams: frequency domain estimation techniques*, CAMS Tech. Rep. 91-25, September, 1991, USC; ASME J. Vibration and Acoustics, to appear.

[BWIS] H.T. Banks, Y. Wang, D.J. Inman and J.C. Slater, *Approximation and parameter identification for damped second order systems with unbounded input operators*, CRSC-TR93-9, North Carolina State University, May, 1993; Control: Theory and Advanced Technology, submitted.

[CA] E.F. Crawley and E.H. Anderson, *Detailed models for piezoceramic actuation of beams*, AIAA Conf. paper 89-1388-CP, 1989, pp. 2000-2010.

[CFW] R.L. Clark, Jr., C.R. Fuller and A Wicks, *Characterization of multiple piezoelectric actuators for structural excitation*, J. Acoust. Soc. Amer., 1991, to appear.

[CR] P. Cawley and R.Ray, *A comparison of the natural frequency changes produced by cracks and slots*, ASME J. Vibration, Acoustics, Stress and Reliability in Design 110 (1988), pp. 366-370.

[DFR] E.K. Dimitriadis, C.R. Fuller and C.A. Rogers, *Piezoelectric actuators for distributed noise and vibration excitation of thin plates*, Proc. 8th ASME Conf. on Failure Prevention, Reliability, and Stress Analysis, Montreal, 1989, pp.223-233.

[DIG] J. Dosch, D.J. Inman, and E. Garcia, *A self-sensing piezoelectric actuator for collocated control*, J. Intell. Material Systems and Structures, 3 1992, pp. 166-185.

[FC] J.L. Fanson and T.K. Caughey, *Positive position feedback control for large structures*, Structural Dynamics and Materials Conf., AIAA Conf. Paper 87-0902, 1987, pp. 588-598.

[IC] A. Isman and K. Craig, *Damage detection in composite structures using piezoelectric materials*, 1st ARO Workshop on Smart Structures and Materials, U. Texas-Arlington, Sept. 22-24, 1993.

[P] P.M. Prenter, *Splines and Variational Methods*, Wiley, New York, 1975.

[S] H. Sato, *Free vibration of beams with abrupt changes of cross-section*, J. Sound and Vibration 89 (1983), pp. 59-64.

[WA] Y. Wang, *Damping Modeling and Parameter Estimation in Timoshenko Beams*, Ph.D. Thesis, Brown University, May 1991.

[W] J. Wloka, *Partial Differential Equations*, Cambridge University Press, New York, 1987.